Sensors and Materials, Vol. 34, No. 12 (2022) 4717–4736
MYU Tokyo

S & M 3139

Economical Inspection Methods Assisted by Unmanned Aerial Vehicle for Bridges in Korea

HyunSang Choi,[1] JaeKang Lee,[1*] and JungOk Kim[2]

[1]Korea Institute of Civil Engineering and Building Technology, Goyang-si 10223, Rep. of Korea
[2]Seoul Institute of Technology, Seoul-si 03909, Rep. of Korea

(Received November 23, 2021; accepted July 21, 2022)

Keywords: bridge, maintenance and inspection, crack detection, water leak, white coating, UAV

Current infrastructure maintenance works face limitations for various reasons: insufficient budget, increasing number of infrastructure facilities requiring maintenance, shortage of labor, and rapidly increasing number of aged infrastructure facilities. To overcome these limitations, a new approach that is different from manual inspection methods under existing rules and regulations is required. In this context, we explored the efficiency of bridge inspection and maintenance using unmanned aerial vehicles (UAVs), which can observe inaccessible areas, be conveniently and easily controlled, and may offer high economic benefits. Various tests were performed on elevated bridges, and suitable UAV images were obtained. The obtained images were inspected using machine vision technology, thereby avoiding subjective evaluations by humans. We also discuss methods for enhancing the objectivity of inspections. Another aim of this study was to automate inspection work and improve work efficiency through computer vision technology. The UAV image analysis and classification technology in this study utilized existing computer vision technology, but the optimization process for each inspection item is described in detail so that it can be directly applied to the inspection task. This is to overcome limitations of current inspection tasks, which require the ability and experience of personnel. For this purpose, objectivity can be secured by optimizing the data acquisition and analysis process on a job-by-job basis. The test results showed that both the efficiency and objectivity of the proposed UAV-based method were superior to those of existing bridge maintenance and inspection methods.

1. Introduction

Bridges are an important example of social overhead capital (SOC). They are directly related to public safety from a socioeconomic perspective and are critical infrastructure components for transport and logistics, which are integral to economic activities. In Korea, the perception of infrastructure safety has significantly dropped in recent years because of natural disasters as well as accidents resulting from human error. Therefore, it is imperative to secure the safety of SOC. Public infrastructure safety is a common concern not only in Korea but also in many other countries that have achieved dramatic economic development over a short period of time. In

*Corresponding author: e-mail: jaekang.lee@kict.re.kr
https://doi.org/10.18494/SAM3739

ISSN 0914-4935

Korea, infrastructure facilities were built mainly during the 1970s and 1980s, when rapid economic development occurred. Infrastructure facilities that were built 30 or more years ago are generally classified as aged infrastructure. Such aged infrastructure facilities accounted for over 11% of all infrastructure facilities as of 2017.[1,2] Therefore, the systematic maintenance, repair, and reinforcement of aged infrastructure facilities, which are integral to securing the national safety network, are critical problems. So far, effective maintenance has kept infrastructure facilities free from accidents. However, the safety of infrastructure may face considerable risk in the future because of the increasing number of aged infrastructure facilities, greater damage inflicted by natural disasters, and inefficient safety and maintenance. Therefore, to ensure infrastructure safety, which is essential for building a prosperous society, future changes must be predicted in a timely manner and new countermeasures must be developed in response.[3–5]

Taking the above in consideration, in this study, we focus on the investigation of inspection measures for bridge infrastructure in Korea. First, we review the current method of bridge maintenance in Korea. Then, we perform an analysis to identify the root cause of the lack of inspection of many infrastructure facilities despite the existence of relevant laws and regulations. On the basis of the analysis results, we discuss the unmanned aerial vehicle (UAV)-image-based inspection of infrastructure facilities as a new approach different from existing inspection methods, which are dependent on subjective and naked-eye inspections. As a demonstration of the proposed UAV-based inspection method, we present the case of an elevated bridge as a test bed. Finally, we perform cost-benefit analysis to evaluate the economic efficiency of the new image-based maintenance method over existing methods.

2. Current Status of Bridge Inspection Methods

2.1 Consideration of bridge maintenance works

As of 2016, there were 30983 bridges in Korea. Among these, 10358 bridges (Types 1 and 2) were registered in the Facility Management System of Korea Infrastructure Safety and Technology Corporation. These bridges are subjected to inspections under two categories, safety inspection and precise safety diagnosis, in accordance with the Special Act on the Safety Control of Installations (full name: Guidelines on Safety Inspection and Precise Safety Diagnosis, Ministry of Land, Infrastructure and Transport) and relevant guidelines on infrastructure safety management. The primary purpose of the safety inspection is to check the current status of infrastructure facilities using simple tools and assess their condition. The safety inspection comprises three sub-inspections: regular inspection, close inspection, and emergency inspection. Close inspection consists of early and regular inspections, whereas emergency inspection consists of damage and special inspections. A regular inspection involves an investigation of the general external condition of accessible areas of the bridge. Manual and assistive tools such as telescopes and mirrors are used, and the inspection is conducted at least once every 6 months. In principle, an early inspection is conducted by a qualified senior engineer who can perform close and emergency inspections, and the initial close inspection of new or modified infrastructure

facilities is conducted within 6 months after the completion of construction or from the date of granting approval for use (including temporary use). A regular close inspection involves an accurate assessment of the current status of infrastructure facilities, an assessment of changes from the initial or previously recorded status, and a confirmation that the infrastructure facilities satisfy the requirements for use. In addition, a closer naked-eye inspection is performed using simple measuring instruments and bridge-specific inspection vehicles if needed. A regular close inspection is conducted at least once every 2 years. Figure 1 shows a photograph of a close inspection using an inspection vehicle.

An emergency inspection is conducted when it is considered necessary by a managing body or when a managing body is requested to do so by the heads of relevant administrations. The emergency inspection is composed of damage and special inspections. A damage inspection is a nonscheduled inspection designed to immediately check the damage to the infrastructure caused by disasters or accidents. A special inspection is conducted at a level similar to a close inspection in cases where a defect such as foundation subsidence or scouring is suspected or where the continuous usability of infrastructure facilities that are prohibited from use needs to be assessed. A precise safety diagnosis is conducted when it is considered necessary to prevent disasters, ensure the safety of infrastructure facilities, and so forth, by a managing body based on the results of a safety inspection. The purpose of a precise safety diagnosis is to check, analyze, and assess the structural safety, causes of defects, and so forth; to identify physical and functional defects in infrastructure facilities; and to adequately and promptly address any problems. Another purpose of the diagnosis is to suggest methods for repair and reinforcement. The features of each bridge inspection type are briefly described in Fig. 2.[(2)]

2.2 Practical limitations in current bridge maintenance works

As explained above, under the Special Act on the Safety Control of Installations, all bridge infrastructure facilities that correspond to Types 1 and 2 are subjected to inspection depending on the period and methods. In this section, implications resulting from the analysis of the current status of general maintenance works, including inspection, are discussed. In this section, we also present the study's background and purpose. Although inspection is mandated by relevant rules

Fig. 1. (Color online) Close inspection using bridge inspection vehicle.

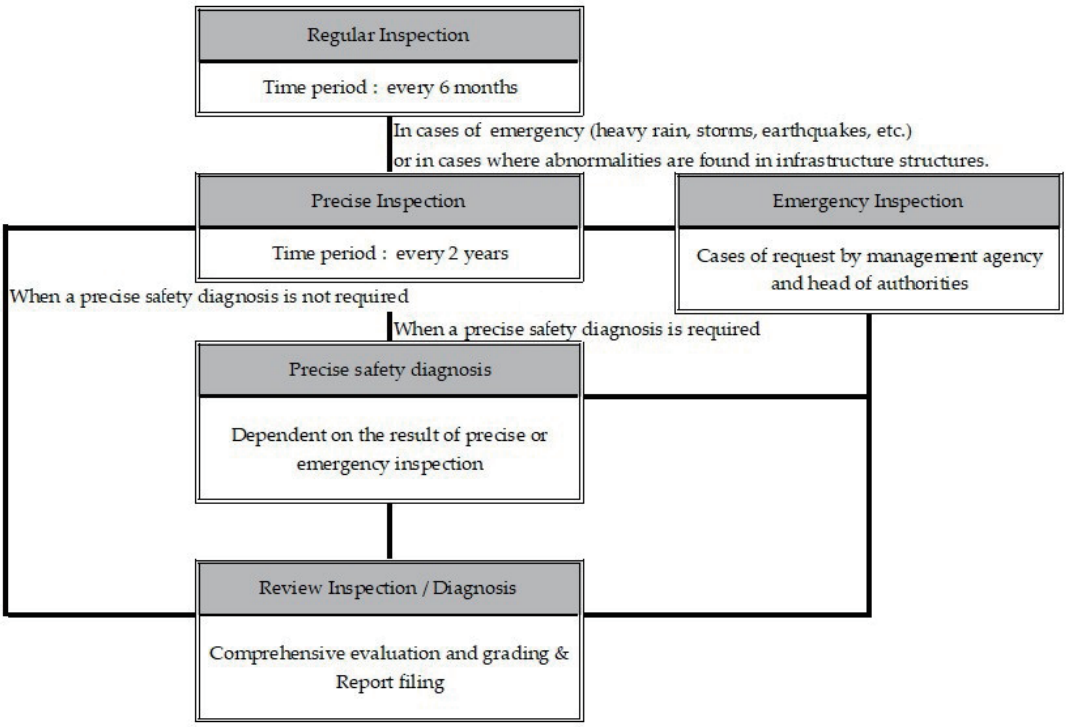

Fig. 2. Bridge inspection procedure.

and regulations, there are many practical difficulties in complying with these rules and regulations. Three main causes of such difficulties were analyzed through a preliminary investigation, as described in detail in the following subsections.

2.2.1 Rapid increase in number and aging of infrastructure facilities

The Korea Expressway Corporation (KEC) expects the total number of infrastructure facilities in Korea to increase by 40% over the next 10 years. The number of bridge infrastructure facilities under the supervision of the KEC was 9180 in 2014, and it is expected to reach 12986 in 2025, an increase of 3806. Furthermore, an increasing number of infrastructure facilities are becoming aged: it is expected that 9576 bridges will be at least 30 years old in 10 years, accounting for approximately 30.9% of bridge infrastructure facilities. Furthermore, 21737 bridges will be in this category in 20 years, accounting for approximately 70.2% of bridge infrastructure facilities. Compared with other countries, infrastructure facilities are aging at a much faster rate in Korea, which is due to its previous rapid economic development in a short period.[(1)]

2.2.2 Shortage of labor

According to an investigation, the average age of the general workforce in the maintenance sector was 44 years as of December 2016. Because the maintenance of infrastructure facilities is viewed as a “dirty, dangerous, and difficult (3D)” job, it is not easy to recruit new workers. Thus,

the industry will face a shortage of labor once the current workforce reaches the age of retirement. The shortage of maintenance workforce with the increasing number of infrastructure facilities implies that the industry, which is heavily dependent on labor, faces a major challenge.

2.2.3 Increase in maintenance costs

The third cause is attributed to the close interrelation between the industry and national policies. A decrease in the SOC project budget leads to a decrease in the infrastructure maintenance budget. In contrast, maintenance costs are expected to increase by 14% on average every year (Table 1). In particular, costs for inspection and diagnosis grew threefold from KRW 111.9 billion in 2014 to KRW 241.6 billion in 2020. This is the budget estimated from the rising number of infrastructure facilities. Despite the increasing maintenance costs due to the increasing number and age of bridges, the national budget for SOC decreased from KRW 22.5 trillion in 2015 to KRW 21.9 trillion in 2016, a decrease of approximately KRW 580 billion.[(2)]

2.2.4 Implications

There are considerable data and evidence to confirm that the current methods of bridge infrastructure inspection face numerous practical challenges. If practical measures are not devised, it would be impossible to conduct an adequate number of inspections in the future because of the decreasing budget and the increasing number of infrastructure facilities. It is therefore necessary to transition from the current labor-based inspections to inspections based on information and communication technology. Recently, geospatial information technologies such as UAV imaging and machine vision have been introduced.[(6–10)] In this study, we therefore investigate whether the active utilization of such technologies can be a feasible solution to the problems described above.

3. Determination of Maintenance Efficiency Through UAV Image Analysis and 3D Viewer

In this section, the possibility of replacing conventional maintenance methods with new methods using UAV images is discussed. To this end, the selection of the study bridge, the UAV operation, UAV image processing, and the characterization of a 3D viewer are explained. Figure 3 shows a flowchart of the processes carried out in this study. In addition, details of the test bed used in this study, the UAV operation, and image matching are described in detail in this section.

Table 1
Increase in maintenance costs.

Note	Budget (0.1 billion KRW)		Annual increase ratio	Increase (times)
	Year of 2014	Year of 2020		
Total	1119	2461	14	2.2
Inspection cost	172	493	19.40	2.9
Improvement cost	273	430	8.10	1.6
Repair cost	674	1538	14.90	2.3

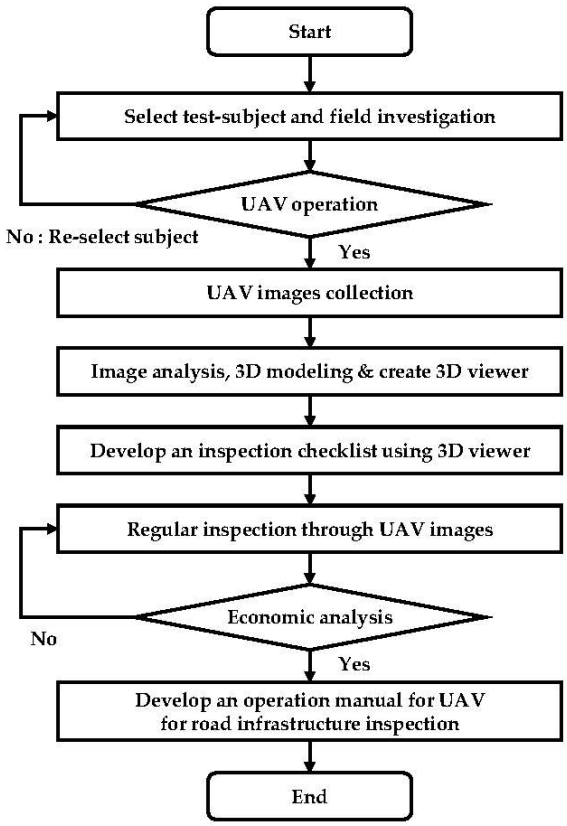

Fig. 3. Flowchart for UAV-based bridge maintenance.

3.1 Introduction of test bed and UAV operation for use

The test bed (bridge infrastructure) selected for the study was Wonjudaegyo Bridge, located in Panbu-myeon, Wonju-si, Gangwondo Province. It was completed in 1995 and is a steel box girder bridge. The bridge has a total of 11 girders, and images were obtained for girders 2–4. Table 2 lists the specifications of the UAV used in the study. This UAV is a model designed specifically for the maintenance of bridges and other infrastructure facilities with an on-top gimbal and is manufactured by Leica.

The UAV was operated for two days between November 20 and December 8, 2016, beginning at 8 a.m. each morning. The operation hours of the UAV were within the hours of minimal traffic around the bridge and minimal temperature fluctuation due to sunrise, which could have resulted in the creation of air currents. Around 500 single images were obtained during the 2 h test operation.

3.2 Establishing flight plan and measuring ground control points (GCPs)

Prior to the operation, the flight trajectory of the UAV was set considering many variables such as the optimal altitude for image recording, camera angle of view, route, duplication rate,

Table 2
(Color online) UAV specifications.

Classification		Description
Maker/name		Leica/Aibotix
Actual image		
Body specifications	Wing	Rotary wing
	Length × width × height	105 × 105 × 45 cm^3
	Flight time	Approximately 25 min
Camera specifications	Resolution	24 MP
	Maximum image size	6000 × 4000
	Takeoff/landing	Vertical
	Gimbal	Three-axis
	Weight	3.4 kg
	Imaging of substructure	Possible (with on-top gimbal)

and direction of sunlight. We used ground control station-based Aibotix software called AiProFlight to set the flight route. Figure 4 shows the UAV flight plan setup.

We installed a total of 11 GCPs. Three GCPs were installed on the bridge deck and the remaining eight were installed directly on the ground below the bridge. The GCPs were measured by virtual reference system (VRS) observation in accordance with aerial photogrammetric regulations. Figure 5 shows the installation points of the GCPs and a photograph taken during installation.

3.3 UAV image processing

PIX4D Mapper software was used to process the obtained UAV images. The international system of WGS94 coordinates was used for the coordinate system, and the variable values of the camera used for recording were considered in the processing. Figure 6 shows a flowchart of the general UAV image processing. Figure 7 shows the outcomes depicted as 3D models generated from the image processing.

4. Analysis of Machine-Vision-Based Inspection Items

Next, we explored technical measures to improve the efficiency of bridge maintenance and inspection using the obtained UAV images and machine vision technology. To this end, a preliminary investigation was conducted on the outcomes derived from an inspector's subjective assessment or items recorded in the inspection log. According to the investigation results, the primary items in the bridge inspection included crack detection, analysis of the white coating formed by water leakage, and a water leakage check. It was confirmed that these items were inspected by subjective assessment. Image analysis was performed in these three major areas of

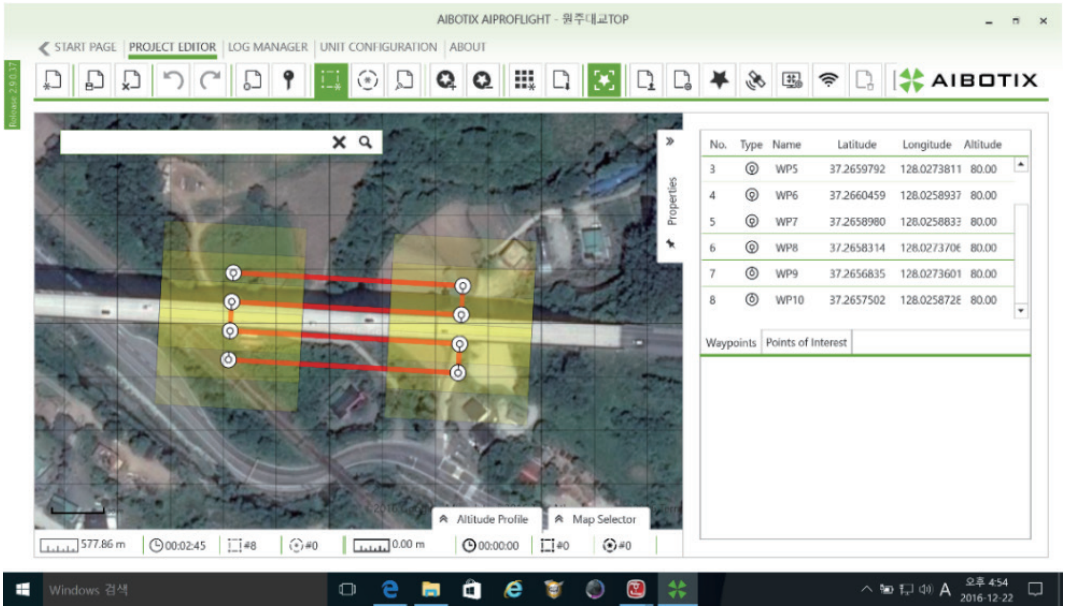

Fig. 4. (Color online) UAV flight plan setup.

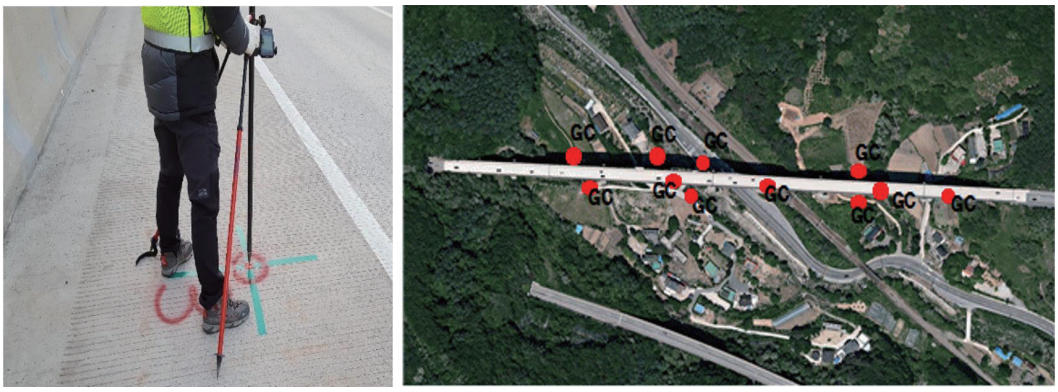

Fig. 5. (Color online) GCP surveying and installation points.

inspection using machine vision technology—the most used technology in the field of image analysis in recent times. Assuming that each item in the inspection can be converted into data and information through analysis and that UAV images can be obtained in a regular and consistent manner, we assumed that automated detection and prediction will be possible through machine learning in the future. This study forms the basic phase of the proposed study plan with the aim of performing the image analysis for each item of inspection subjected to UAV imaging.

4.1 Machine-vision-based UAV image analysis

As explained above, specific software was developed to support the bridge inspection through machine vision technology for single images obtained by the UAV (Fig. 8). This software developed in C++ imports images of bridge members, creates an algorithm for

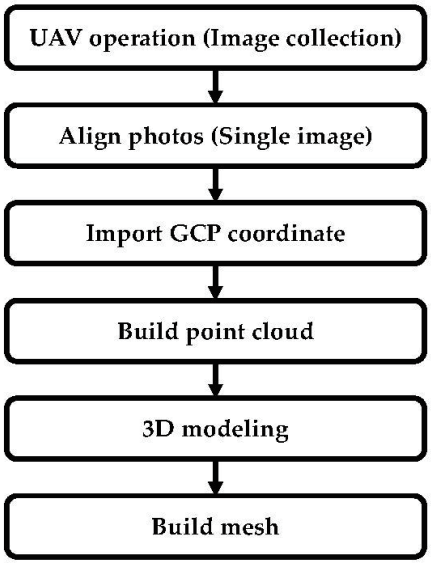

Fig. 6. Process for image matching.

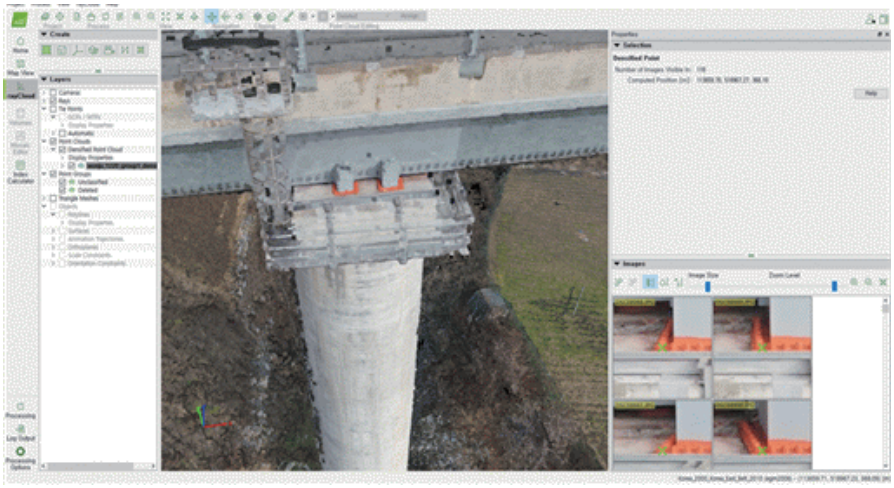

Fig. 7. (Color online) Results of image matching.

inspection as a function, and finally displays the corresponding inspection results on each input image, which can be printed as the output.

This process was mainly divided into two parts. The first part extracts the information channels required prior to image analysis, and the second part applies the algorithm required to extract candidates for inspection. The first step of the inspection of the items (crack, white-coated, and water leakage) for analysis was to convert the color format, which was carried out for all three major inspection items. The Lab color space was formed by nonlinearly converting the International Commission on Illumination (CIE) XYZ color spaces in accordance with the antagonism theory of human color vision.[11] The Lab color space represents the color space of CIE 1976 Lab, which consists of a three-channel color format (L for lightness, i.e., brightness,

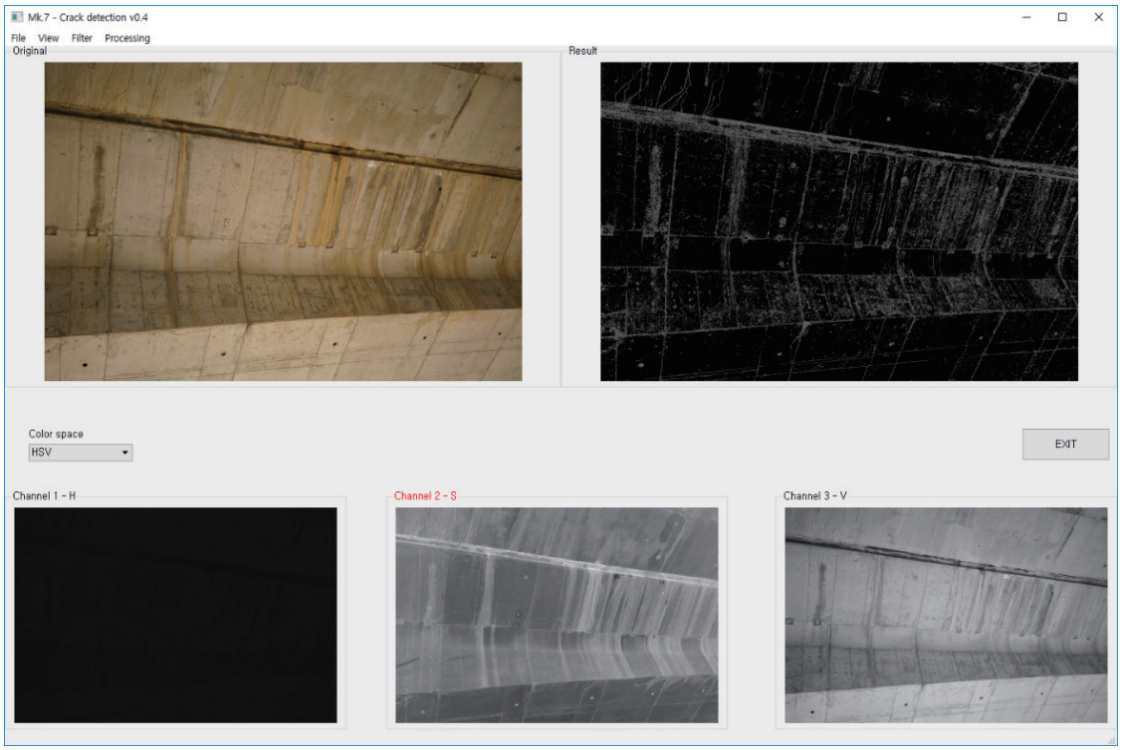

Fig. 8. (Color online) Development of bridge inspection software based on UAV images.

and a and b for the green–red and blue–yellow color components, respectively) and is used by converting the CIE XYZ color space. This transformation is based on a cubic function, and the Lab color space has a nonlinear relationship with the actual wavelengths of light. In other words, the gap between two different colors is designed to be proportional to the actual chrominance perceived by human sight. The formal conversion of the Lab color format is performed as follows:

$$L^* = 116 f\left(\frac{Y}{Y_n}\right) - 16\,, \tag{1}$$

$$a^* = 500\left(f\left(\frac{X}{X_n}\right) - f\left(\frac{Y}{Y_n}\right)\right), \tag{2}$$

$$b^* = \square \quad \left(f\left(\frac{Y}{Y_n}\right) - f\left(\frac{Z}{Z_n}\right)\right). \tag{3}$$

Here, $f(t)$ is

$$f(t)=\begin{cases} t^{1/3} & \text{if } t>\left(\dfrac{6}{29}\right)^3 \\ \dfrac{1}{3}\left(\dfrac{29}{6}\right)^2 t+\dfrac{4}{29} & \end{cases}, \tag{4}$$

where X_n, Y_n, and Z_n are the normalized values of CIE XYZ for the standard white color.

The inverse transformation is performed as follows:

$$Y=Y_n f^{-1}\left(\frac{1}{\square}\left(L^*+16\right)\right), \tag{5}$$

$$X=X_n f^{-1}\left(\frac{1}{116}\left(L^*+16\right)+\frac{1}{500}a^*\right), \tag{6}$$

$$Z=Z_n f^{-1}\left(\frac{1}{116}\left(L^*+16\right)-\frac{1}{200}b^*\right), \tag{7}$$

$$f^{-1}(t)=\begin{cases} t^3 & \text{if } t>\dfrac{6}{29} \\ 3\left(\dfrac{6}{29}\right)^2\left(t-\dfrac{4}{29}\right) & \end{cases}. \tag{8}$$

Following the first step of the analysis performed for the difference in brightness, Gaussian adaptive filtering was applied to extract the priority candidates for each inspection item in relation to these images, then the binarization process was carried out. Binarization is the most commonly used solid segmentation method. It is frequently used to divide an image to extract a desired area or a specific object in the image, making it suitable for our application. In the binarization, the original image was converted into a grayscale image, and the background and objects were separated using threshold values. In the application, threshold values were applied to the fixed area of the entire image. The grayscale image was then inputted to scan the entire image. If the pixel value was greater than the threshold value, the pixel value at the same position in the resulting image was assigned a white color; otherwise, the value was assigned a black color.

4.2 Analysis for crack detection

In the image of the bridge, cracks were generally indicated in a darker color than the other areas. To use this feature, the color format conversion was carried out in the first step (Fig. 9). The recorded image was in RGB color format, which was then changed to Lab color format. To use channel L, data were extracted from channel L in the second step. The extracted channel L

data were then used in three different methods (Fig. 10). First, the Gaussian adaptive threshold method was applied to the channel L data. In this method, the area-weighted average is calculated by using the Gaussian load within the local area as the threshold value. Cracks had lower lightness values than the other areas, and areas with a lightness value below the threshold value were designated as candidate areas. With regard to the set value for the Gaussian adaptive threshold, the size of the local area was set as 45 × 45 for experimental reasons. The binary images obtained with the threshold produced crack candidate 1 (Fig. 11).

In the second method, the contour of the area was extracted using the channel L data. When extracting the contour, the area was detected on the basis of the similarity of the lightness value and extracted by setting the data on the contour of the identical area as boundaries. Then, for the extracted area boundaries, when the width of the area was below the threshold value, the detected area was considered to be false or inaccurate (because of noise in the image, etc.) and was then removed. The resulting image is shown in Fig. 11. The data for the area extracted through the two steps were used as crack candidate 2 (Fig. 12).

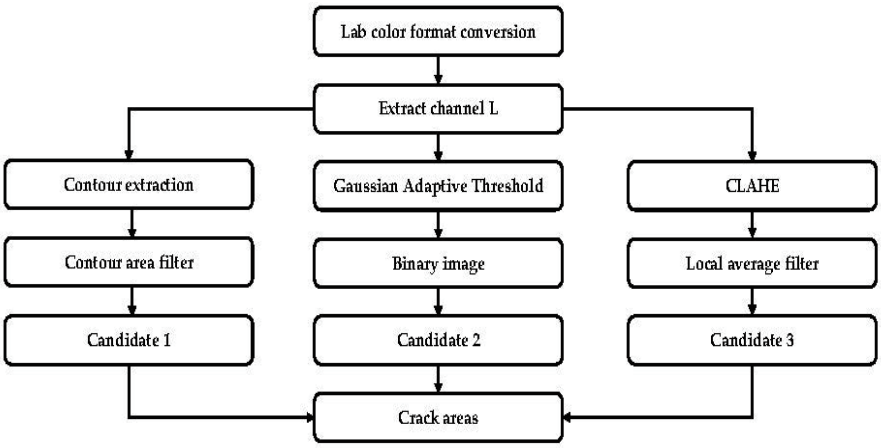

Fig. 9. Flowchart for crack detection.

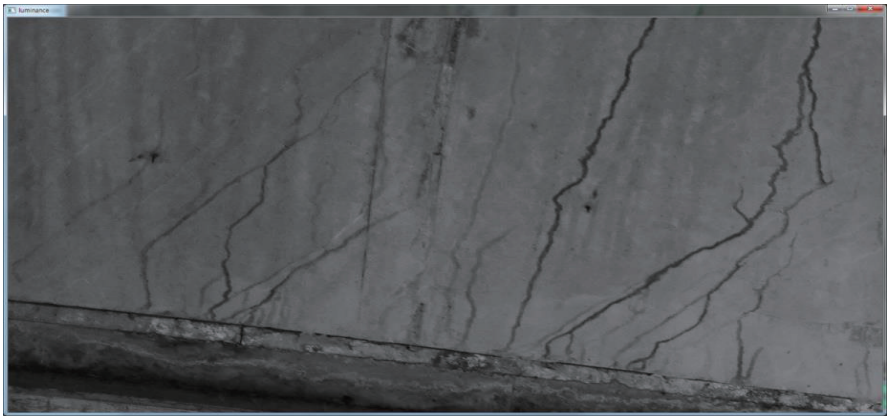

Fig. 10. Data extracted from channel lightness (L).

Fig. 11. Image obtained using Gaussian adaptive threshold method.

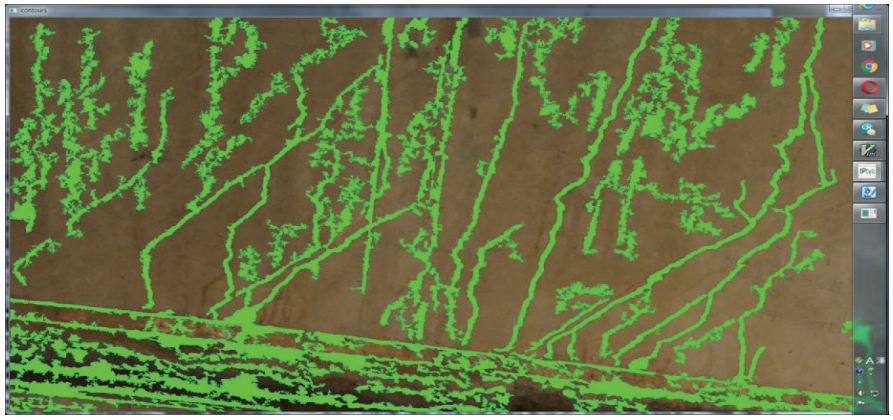

Fig. 12. (Color online) Image obtained by extracting area boundaries.

In the third method, histogram equalization was carried out using contrast-limited adaptive histogram equalization (CLAHE) to minimize the effects of external lightness. CLAHE was used because it can minimize the impact of the difference in regional illumination when carrying out histogram equalization. A local average filter was applied to each area of the image obtained from histogram equalization to compare the average lightness and the current pixel lightness. A darker image was detected by comparing all pixels with the local average, which was designated as crack candidate 3 (Fig. 13).

After extracting crack candidates 1, 2, and 3, all the detected intersections in each candidate were measured. Finally, the areas with boundaries greater than or equal to a certain width and the areas with darker values than the surrounding areas were assumed to be cracks. The crack detection result (Fig. 14) was verified on the basis of the inspector's on-site assessment and by direct comparison. This verification was conducted because the inspection result was based on the naked-eye observation by inspectors as mandated by the current regulations. One of the objectives of this study was to improve the objectivity of the inspection, which is dependent on the subjective assessment of inspectors, and explore such a possibility through comparative analysis. Therefore, only the cracks with a width of 0.5 mm or greater were taken into

Fig. 13. Image obtained after applying local average filter.

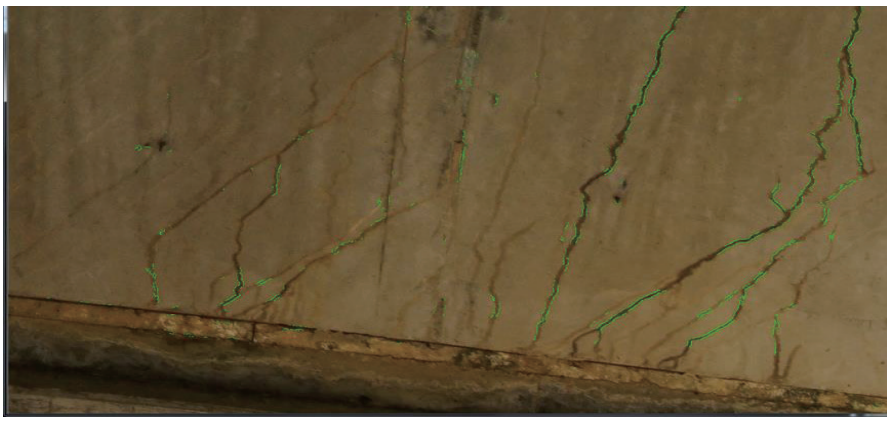

Fig. 14. (Color online) Image obtained from crack detection.

consideration, and the comparison was carried out in only a quarter span of the lower part of the bridge.

4.3 Analysis of water leakage

To detect a water leakage in the image, the data for the L channel were again used as the primary data (Fig. 15). The leak area also has lower lightness values than the other areas. Therefore, to detect the leak area, the channel L data, which indicate the lightness in the Lab color format, were extracted in the first step (Fig. 16). The data extracted from channel L were then used in two different methods, i.e., Canny edge detection and Gaussian adaptive threshold. In the first method, the data representing the edges in the image were extracted using the Canny edge detection algorithm. For the edges in the bridge image, the threshold values were set as 0 and 150 for experimental purposes, and the resulting images shown in Figs. 17 and 18 were obtained. Because the data representing the edges included data for all the edges in the image, a top-hat morphological filter with a filter kernel of size 5 × 5 was applied to detect the edges of the darker area. Figure 19 shows the edge image to which the filter was applied, and the image was then used as leak candidate 1. In the Gaussian adaptive threshold method, binary images

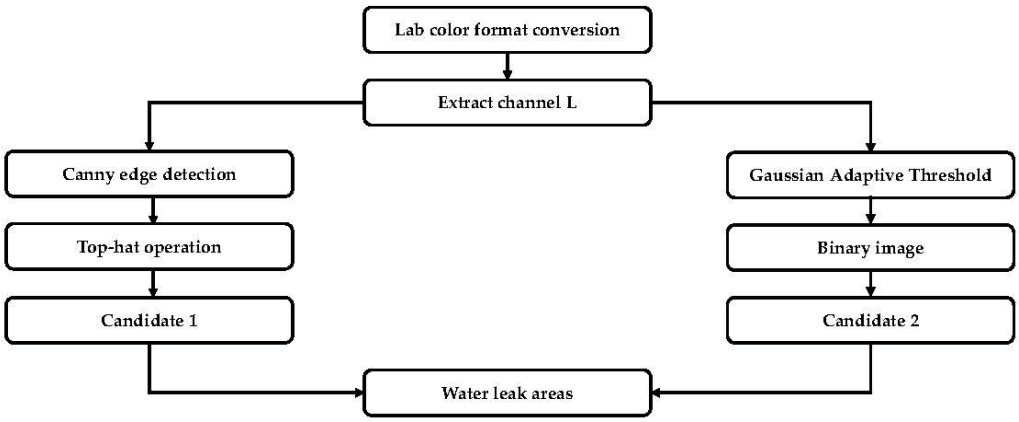

Fig. 15. Flowchart for water leakage detection.

Fig. 16. Channel L data.

Fig. 17. Image obtained from Canny edge detection.

were extracted using the same method as in the crack detection. Darker areas were detected in the binary images to obtain the image shown in Fig. 20, which was used as leak candidate 2.

The intersection of the areas detected in leak candidates 1 and 2 was measured, and the leak areas with lower lightness values than the surrounding areas and the edges in the darker areas were detected in the final step. The resulting image is shown in Fig. 20.

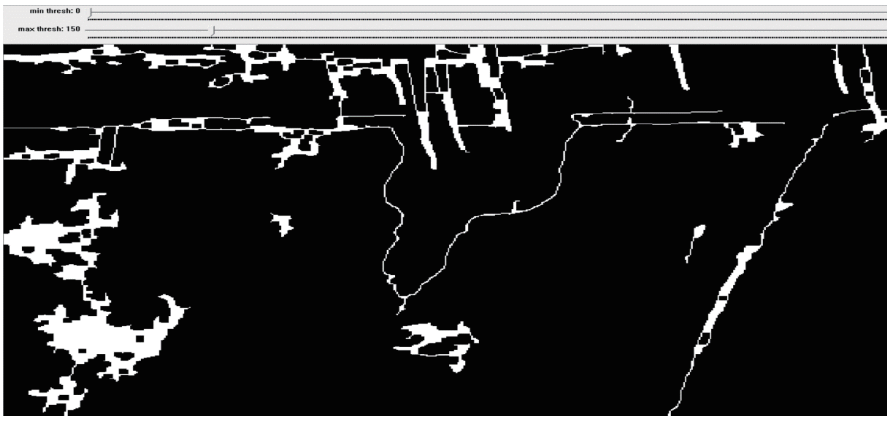

Fig. 18. Image obtained from top-hat orphological operation.

Fig. 19. Image obtained from Gaussian adaptive threshold method.

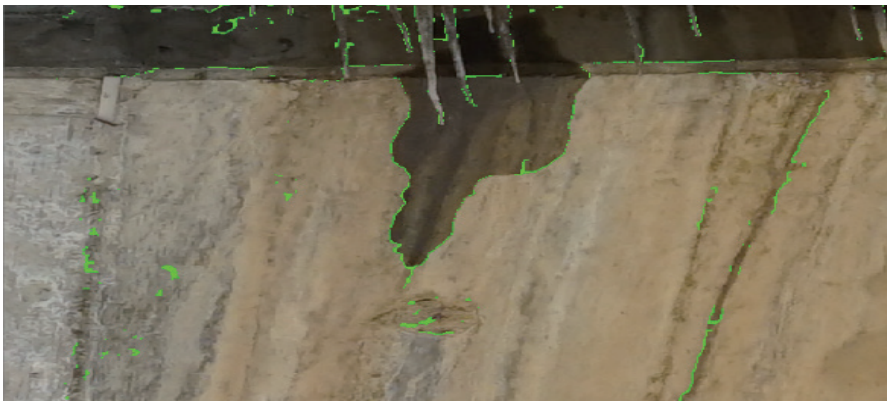

Fig. 20. (Color online) Image obtained from water leakage detection.

4.4 Analysis of white-coated (efflorescence) detection

The white-coated area in the bridge image had higher lightness values than the surrounding areas. To use this feature, as in the cases of crack and leak detection, the channel L data were

obtained from the Lab color format in the first step (Fig. 21). As in the other cases, Canny edge detection and the Gaussian adaptive threshold method were used in the second step.

Figure 22 explains the first step for extracting channel L from Lab color format. When whitecoating occurred, more edges were found in the efflorescence area than in the other areas. Therefore, the edges were detected through Canny edge detection from Fig 23. The detected edges were designated as efflorescence candidate 1, as shown in Fig. 24. As the efflorescence area had higher lightness values than the surrounding areas, the data were extracted only when the value exceeded a threshold value, and a binary image was obtained by another method, as shown in Fig. 25. This image was designated as efflorescence candidate 2. Then, the intersection of efflorescence candidates 1 and 2 was measured, and the efflorescence areas with higher lightness values than the surrounding areas as well as many edges within the efflorescence areas were detected in the final step. The detected efflorescence areas are shown in Fig. 25.

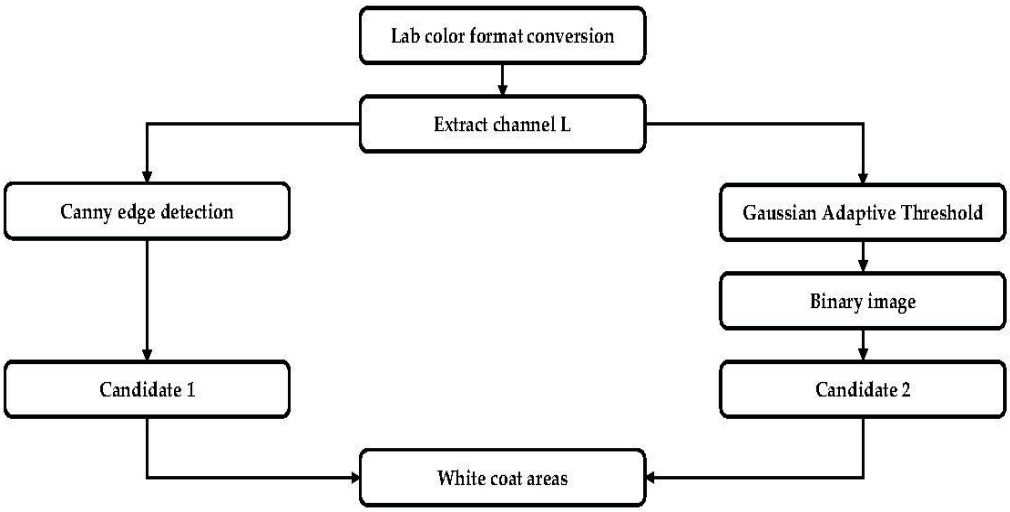

Fig. 21. Flowchart for white-coated area detection.

Fig. 22. Channel L data.

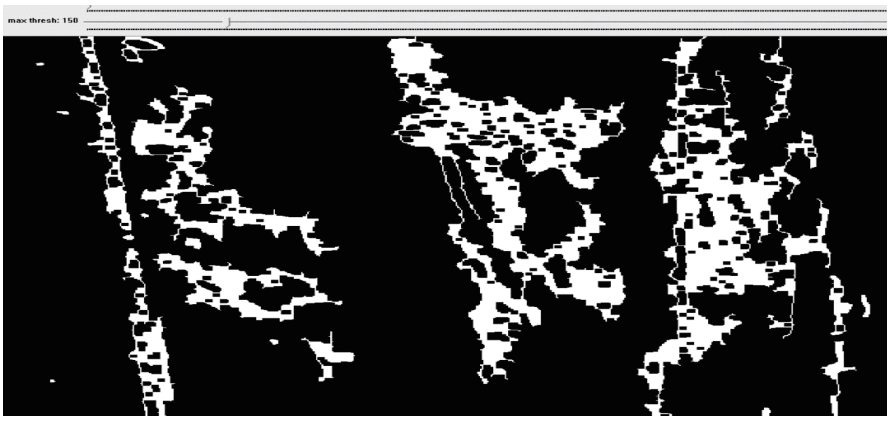

Fig. 23. Image obtained from Canny edge detection.

Fig. 24. Image obtained from Gaussian adaptive threshold method.

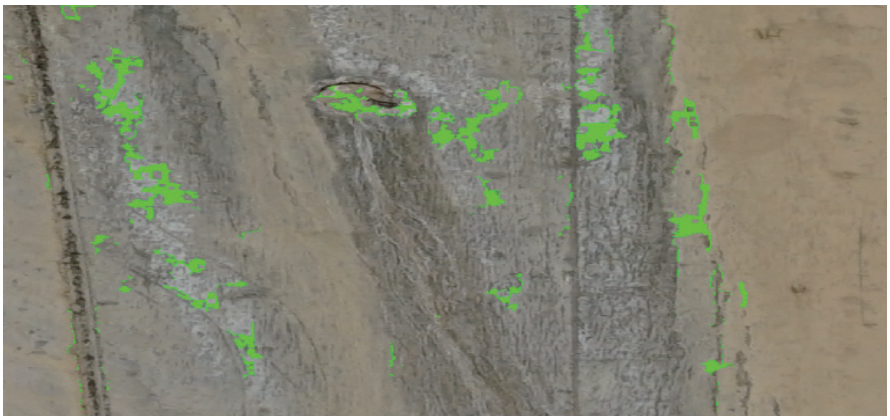

Fig. 25. (Color online) Image obtained from white-coated detection.

4.5 Cost-benefit analysis and implications

The computer vision technology described above was effectively applied to bridge inspection.[12] This result was confirmed by field technicians performing on-site inspections, but

Table 3
Details of cost-benefit analysis.

Work process	Method	Duration	No. of staff	Cost (in KRW)
Pylon inspection	Existing methods	1 day	3–4	Labor cost (4 staff): 600000/day Equipment rental cost (18-ton crane): 1 million/day
	Drone	2 h	2	Labor cost (2 staff): 400000/day Equipment rental and photography: 500000–1 million/day (depending on work conditions)
Pier inspection	Existing methods	2 days	3–4	Labor cost (4 staff): 600000/day Equipment rental cost (18-ton crane): 1 million/day
	Drone	4 h	2	Labor cost (2 staff): 400000/day Equipment rental and photography: 1 million/day (depending on work conditions)
Bridge bearing inspection	Existing methods	3 h	5–6	Labor cost (4 staff): 600000/day Equipment rental cost (bridge inspection car): 1.5 million/day
	Drone	1 h	2	Labor cost (2 staff): 600000/day Equipment lease: 1 million/day (depending on work conditions)

the number of technicians was not sufficient to quantify the result. Accordingly, further study is required to validate the technology.

The results of this study show that the proposed UAV image acquisition and analysis method for inaccessible bridge members overcomes the limitations of the existing bridge inspection methods and thus may successfully replace them. To confirm this possibility, a cost-benefit analysis was performed, whose details are listed in Table 3.

For the cost-benefit analysis, particular personnel were selected because of the characteristics of the target bridge. The cost-benefit analysis for a single bridge cannot be extended to every bridge. In particular, because Wonjudaegyo Bridge, the target bridge in this study, is an elevated bridge, our analysis might produce many unavoidable differences.[13] When an elevated bridge is inspected, inaccessible members such as the pylon, pier, and bridge bearing always require an inspection car and a crane. The cost for existing methods that use such equipment is two or three times that for the UAV-based inspection method, and the existing methods also require more working hours. Moreover, because the UAV system is easier to transport and install, two or more bridges can be inspected in a single day, thereby increasing its advantageousness.

5. Conclusions

We investigated maintenance and inspection measures for bridge infrastructures with the aim of increasing their efficiency. Korea is facing the problem of simultaneous deterioration of many infrastructure facilities because of its previous rapid economic development in a short period. The shortage of labor for maintenance and inspection is also aggravating the situation. In addition, the maintenance budget is decreasing along with its importance in policy agendas. Considering this background, the current maintenance and inspection methods have clear limitations, which threaten public safety.

We considered the use of a UAV, which has advantages in terms of economy, convenience, and data acquisition in inaccessible areas, as an alternative to existing methods. We selected Wonjudaegyo Bridge as the test bed and used a Leica Aibotix rotary-wing UAV for inspection. The images obtained by the UAV were displayed in a 3D viewer after an image matching process. Thus, the maintenance analysis can be carried out regardless of location with Internet. Machine vision technology, which is currently one of the most widely used image analysis technologies, was applied to inspect the matched images. Crack detection, efflorescence analysis, and a leak check were carried out, and the results were analyzed on the basis of the bridge inspection list. We also developed software that included functions for each elemental technology to monitor the UAV-based maintenance and inspection of bridges. Finally, a cost-benefit analysis was performed to compare the UAV-based inspection method with existing methods. The proposed UAV-based method was found to be superior in terms of economy, convenience, and objectivity.

Acknowledgments

This study was conducted under the research project Development of Digital Safety Watch Technology for Old Buildings in Metropolitan Units (RS-2022-00142434) funded by the Ministry of Land, Infrastructure and Transport (MOLIT) and the Korea Agency for Infrastructure Technology Advancement (KAIA). We would like to thank the members of the research team, MOLIT, and KAIA for their guidance and support throughout the project.

References

1 K. H. Park and J. W. Sun: J. Korea Acad.-Ind. Coop. Soc. **16** (2015) 7893. https://doi.org/10.5762/KAIS.2015.16.11.7893
2 K. H. Park and J. W. Sun: J. Korea Acad.-Ind. Coop. Soc. **17** (2016) 13. https://doi.org/10.5762/KAIS.2016.17.10.13
3 N. Metni and T. Hamel: Autom. Constr. **17** (2007) 3. https://doi.org/10.1016/j.autcon.2006.12.010
4 J. Oh, G. Jang, S. Oh, J. H. Lee, B. Yi, Y. S. Moon, J. S. Lee, and Y. Choi: Autom. Constr. **18** (2009) 929. https://doi.org/10.1016/j.autcon.2009.04.003
5 A. Mohan and S. Poobal: Alexandria Eng. J. **57** (2018) 787. https://doi.org/10.1016/j.aej.2017.01.020
6 P. Prasanna, K. Dana, N. Gucunski, and B. Basily: Proc. SPIE, Sensors and Smart Structures Technologies for Civil, Mechanical, and Aerospace Systems **8345** (2012) 834542. https://doi.org/10.1117/12.915384
7 R. S. Adhikari, O. Moselhi, and A. Bagchi: Autom. Constr. **39** (2014) 180. https://doi.org/10.1016/j.autcon.2013.06.011
8 G. Li, S. He, Y. Ju, and K. Du: Autom. Constr. **41** (2014) 83. https://doi.org/10.1016/j.autcon.2013.10.021
9 R. S. Adhikari, O. Moselhi, A. Bagchi, and A. Rahmatian: J. Comput. Civil Eng. **30** (2016) 04016004. https://doi.org/10.1061/(ASCE)CP.1943-5487.0000566
10 G. Li, X. Zhao, K. Du, F. Ru, and Y. Zhang: Autom. Constr. **78** (2017) 51. https://doi.org/10.1016/j.autcon.2017.01.019
11 Wikipedia Lab color space: https://en.wikipedia.org/wiki/Lab_color_space (accessed 16 March 2018).
12 J. Irizarry and E. N. Johnson: Georgia Inst. Technol. (2014). http://hdl.handle.net/1853/52810
13 J. K. Lee, M. J. Kim, J. O. Kim, J. S. Kim, T. D. Acharya, and D. H. Lee: Gi4DM (Geoinformation for Disaster Management) Proc. **4** (2019) 23.